Thin Solid Films 519 (2011) 2867–2869

Contents lists available at ScienceDirect

Thin Solid Films

journal homepage: www.elsevier.com/locate/tsf

Phase-modulated ellipsometry for probing the temperature-induced phase transition in ruthenium-doped lead zinc niobate–lead titanate single crystal

Chun-I Chuang [a], Vera Marinova [b], Shiuan-Huei Lin [c], Yu-Faye Chao [a,*]

[a] Department of Photonics and Institute of Electro-Optical Engineering, National Chiao Tung University, 1001 University Rd., Hsinchu, Taiwan 300, ROC
[b] Central Laboratory of Optical Storage and Processing of Information, Bulgarian Academy of Sciences, P.O. Box 95, 1113 Sofia, Bulgaria
[c] Department of Electrophysics, National Chiao Tung University, 1001 University Rd., Hsinchu, Taiwan 300, ROC

ARTICLE INFO

Available online 20 December 2010

Keywords:
Refractive index
Perovskite
Curie region
Ellipsometry

ABSTRACT

Phase-modulated ellipsometry was applied to measure changes in the refractive index of pure and ruthenium (Ru)-doped 0.9Pb $(Zn_{1/3}Nb_{2/3})O_3$ (PZN)–0.1$PbTiO_3$ (PT) during the heating process in real time. Both samples were heated from room temperature to 200 °C in a thermally insulated chamber. In both samples, the phase transitions were observed to change from tetragonal to cubic. The temperature region at which the phase transition (Curie region) of Ru-doped 0.9PZN–0.1PT occurred not only broadened but also shifted to a lower temperature. The refractive indices were extremely stable in this region, meaning that Ru-doped 0.9PZN–0.1PT is a more favorable medium for the fabrication of optical memories.

1. Introduction

Within the past few decades, the complex perovskite-type ferroelectric materials (with the general formula ABO_3) have found numerous applications [1]. The perovskite materials are attractive because they exhibit extremely high piezoelectric coefficients and a wide region of controlled dielectric constants when the compositions are near the morphotropic phase boundary (MPB) [2–4]. Kuwata et al. [5] successfully grew mixed crystals between the relaxors $Pb(Zn_{1/3}Nb_{2/3})O_3$ (PZN) and the ferroelectric $PbTiO_3$ (PT). It is worth noting that the structures of PZN and PT under ambient conditions are rhombohedral and tetragonal [6,7], and the piezoelectric effect of the $(1-x)$PZN–xPT single crystals near the MPB (x~0.1) is the greatest ever observed [5,8]. Cox et al. [9] found another orthorhombic phase around the MPB between the rhombohedral and tetragonal phases. The rhombohedral-orthorhombic boundary is near-vertical [10]. This boundary is similar to the rhombohedral-monoclinic boundary observed in the $PbZn_{1-x}Ti_xO_3$ (PZT) system [9].

The phase structures of PZN–PT near the MPB vary from orthorhombic (ferroelectric, FE) to tetragonal (FE), then to cubic (paraelectric, PE) under heating [9,10]. The relaxor ferroelectric materials exhibit anomalies in the dielectric response over a wide region near the FE-PE transition temperature, normally called the Curie region. This phenomenon is caused by either spatial fluctuation of the B-site cations or the diffuse phase transition (DPT) [11]. The dielectric, pyroelectric, elastic-electric, and optoelectric properties of ferroelectric materials are all significantly enhanced in the Curie region [12,13].

In previous studies, it has been found that doping Ru into complex oxides can enhance the photorefractive effect in the red and near-infrared spectral regions [14–17]. In addition, using Ru as a dopant in various inorganic crystals can considerably improve their response time and photoconductivity [18–20]. Therefore, Ru-doped perovskites can be considered a practical material for optical memories. Since there is no related information about the refractive indices of Ru-doped PZN–PT during heating/cooling process, we measure their refractive indices during heating in order to understand what would be the most favorable working temperature for optical storage.

Ellipsometry is an effective measurement technique because it is sensitive, fast and non-destructive. Consequently, ellipsometry has been widely applied in many different fields such as for the fabrication of optical coatings, data storage, semiconductors, flat panel displays, biotech, etc. The technology of phase-modulated ellipsometry (PME) was developed by Jasperson et al. [21] and later improved by Acher et al. [22]. As a remarkable progress in the semiconductor and mechanical industry, PME is greatly improved and applied to real time measurement. The phases of the perovskite materials are temperature dependant, which makes PME a powerful technique to study dynamic changes in the phase transition. In this study, we applied PME to measure changes in the refractive index of pure and Ru-doped 0.9PZN–0.1PT during the heating process. To avoid the noise from direct current (DC) signals, which can affect the measurement of the ellipsometric parameter Ψ [23,24], we averaged the DC signals every 0.1 s. It is easy to obtain the refractive index n_0 of a bulk medium in real time by substituting the measured Ψ and Δ into the bulk model of an isotropic medium [25].

* Corresponding author. Tel./fax: +886 3 5731914.
E-mail address: yfchao@mail.nctu.edu.tw (Y.-F. Chao).

0040-6090/$ – see front matter © 2011 Elsevier B.V. All rights reserved.
doi:10.1016/j.tsf.2010.12.085

2. Experiments

2.1. Phase-modulated ellipsometry (PME)

The schematic setup of the PME is shown in Fig. 1. The strain axis of the PEM (HINDS PEM-90/CF50) was set at 0° [26], and the azimuths of the polarizer and analyzer were positioned at −45° and 45°, respectively, with respect to the incident plane, by using the alignment technique [26]. The modulation amplitude (δ_0) of the PEM was calibrated [27] and adjusted to be 2.4065, setting $J_0(\delta_0)$ equal to zero during the measurements. The HeNe laser (632.8 nm) was used as a probe beam. Its beam diameter was approximately 2 mm. The light transmitted through the PEM was incident on the sample at 70°. The modulated intensities were obtained by the amplified photodetector (PDA55, Thorlabs) through the data acquisition system (BNC 2110 and PCI 6115, National Instruments, 4 channels). The acquired data was decomposed into the DC and harmonic signals by the multi-channel virtual lock-in amplifier, which was programmed with LABVIEW. The physical parameters of the measured medium could then be deduced in real time. We achieved a rate of 10 sets/s in this research.

2.2. Temperature control

The samples were heated from room temperature to 200 °C within approximately 40 min in a thermally insulated chamber. The chamber is comprised of a glass fiber box with a cover, as shown in Fig. 1. The thermoelectric cooler (TE cooler) operates based on the Peltier effect, so can be used as heater when the electric current is inversely applied. The TE cooler is small but highly reliable. The sample was sandwiched between two TE coolers to maintain uniformity of temperature of the sample. A k-type thermocouple was attached to the surface of the sample to monitor the temperature. The voltage produced by the thermocouple was acquired by one of the channels of the same data acquisition system. The voltage was then converted to the required temperature scale according to the NIST ITS-90 Thermocouple Database. In this way, both the temperature and the ellipsometric parameters could be simultaneously monitored.

2.3. Materials

Thick glass (~3 mm, BK7) was used to insure insulation of the chamber under heating. The glass is thick enough to separate the reflected light from the second surface under the incident angle of the probe beam was at 70°, in such case the bulk model can be used to deduce its refractive index. The refractive index was measured under the same circumstances as for measurement of the perovskites. After testing the heating effect with the glass, we probed pure and Ru-doped 0.9PZN–0.1PT which were developed by Scholz et al. [28]. Both samples were cut into a wedge shape along the [1 1 1] direction. The samples were around 4×4 mm^2 in size and 1 mm thick. This meant that multiple reflections could be avoided.

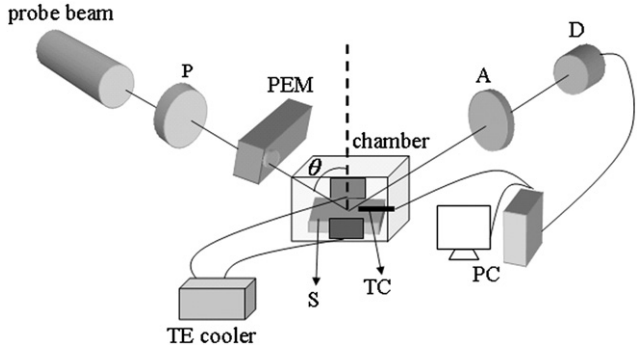

Fig. 1. Schematic setup of the PEM ellipsometer for measuring the variation in the refractive index during the heating process: probe beam: HeNe laser (632.8 nm); P: polarizer; PEM: photoelastic modulator; S: sample; θ: incident angle = 70°; A: analyzer; D: photodiode detector; PC: personal computer; TC: K type thermocouple.

3. Experimental results and discussion

As mentioned in the Handbook of Ellipsometry, the DC term measured by the PME can be averaged every 100 cycles of modulation of the phase modulator to reduce noise [23]. In our system, the sampling rate and the buffer size of the DAQ card were set at 454 kHz and 51,200 data size for recording the intensity measurements. The intensity was acquired and saved in the buffer. Then 45,400 data points were extracted from the buffer. The DC and harmonic terms were obtained by power spectrum analysis and virtual lock-in amplifier, respectively. In other words, the DC and the harmonic terms were averaged every 5000 cycles of the modulated intensity in this PME. In this way, 10 sets/s of ellipsometric parameters Ψ and Δ could be measured. For convenience, we displayed the deduced refractive index and measured temperature on line. Theoretically, the DC and harmonic signals could be averaged every 100 cycles instead of every 5000 cycles which would improve the speed of measuring the refractive index to 500 sets/s. However, the measuring speed is limited by the speed of data transfer between the multi-channels of the DAQ system and the computer.

The refractive indices of BK7 before and during the heating process were 1.513 ± 0.001 and 1.513 ± 0.002. This standard deviation in the refractive index is close to the limit of the ellipsometry [29]. Through this experiment, we can prove that the temperature effect to the PEM [30] has been eliminated. This gives us enough confidence to measure the refractive index of the perovskites under heating with this system.

The refractive indices of pure and Ru-doped 0.9PZN–0.1PT during the heating process are plotted against temperature, as shown in Figs. 2 and 3, respectively. The maximum changing rate of refractive index is on the order of 10^{-4}/s, which is much slower than the measuring speed (10 sets/s). Although the exact phases of the samples cannot be determined by our system, one can clearly distinguish the phase transitions from the variation in the refractive indices. The Curie region can be clearly observed in both pure and Ru-doped 0.9PZN–0.1PT, but in the doped PZN–PT that region not only shifted to a lower temperature but was broadened by a factor of 2.5 with respect to that of pure PZN–PT. The phase diagram of pure PZN–PT has already been widely studied [9,10]. The changes in phase structure of this newly fabricated Ru-doped 0.9PZN–0.1PT during heating proved

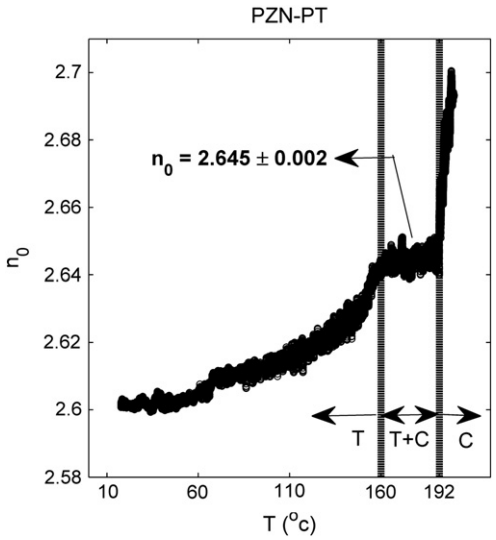

Fig. 2. Refractive indices of pure 0.9PZN–0.1PT against temperature during heating: T: tetragonal; C: cubic.

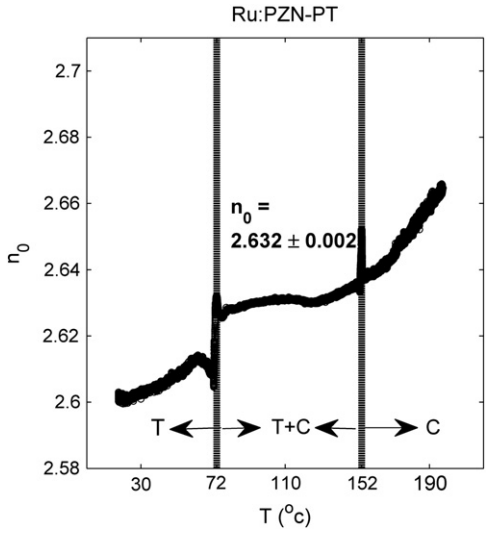

Fig. 3. Refractive indices of Ru-doped 0.9PZN–0.1PT against temperature during heating: T: tetragonal; C: cubic.

to be a very interesting problem. In Scholz's study [28] on the phase structures of pure and doped PZN–PT at room temperature, they concluded that the most probable average phase structures of both materials are tetragonal. Based on this conclusion, we assume that the average phase structures of doped and undoped PZN–PT are the same, even during the heating process. By comparing the phase diagram for $(1-x)$PZN–xPT [9,10], we mark the phase transitions; see Figs. 2 and 3.

In the process of storage, the temperature of the surroundings can fluctuate due to laser irradiation, heat dissipation, etc. However, for optical storage, the refractive index of the perovskite material must be stable under the working temperature. Using real time measurement by PME, we find that undoped 0.9PZN–0.1PT has a stable refractive index (2.645 ± 0.002) within the Curie region (160 °C to 192 °C). Above the Curie temperature (T_c), the structure starts to change from hybrid tetragonal and cubic phase into pure cubic phase. In Fig. 2, one can observe that T_c is 192 °C, which is comparable to what is found for different concentrations in previous studies [9,10,31]. Due to the limitation of this instrument, the refractive indices increased sharply above T_c without the expected peak [31]. Although the refractive indices of pure 0.9PZN–0.1PT are high and stable within the Curie region, this region is still much higher than room temperature. Therefore, efforts have been made to reduce and broaden the temperature throughout this region in order to provide a more practical storage medium. In general, the distribution of the Curie region as well as T_c can be changed by doping some elements into the A-site or B-site of Pb-based perovskites [11,32–35]. We observed this phenomenon in the Ru-doped 0.9PZN–0.1PT, as shown in Fig. 3. The refractive indices of the doped PZN–PT are 2.632 ± 0.002 in the Curie region, while the temperature range shifted from 160 °C to 192 °C down to 72 °C to 152 °C. This shifting and broadening of the Curie region makes the Ru-doped 0.9PZN–0.1PT more suitable for infrared or even red light sources in optical storage. The reduction in T_c may result from: (1) the more delocalized 4*f* orbital with itinerant t_{2g} of Ru can aid the exchange coupling interaction [35]; and (2) doping larger B-site ions can narrow the electronic bandwidth [36,37]. A previous study [28] concluded that Ru^{4+} could be substituted for Ti^{4+} when doping Ru into PZN–PT. The ionic radii of Ru^{4+} and Ti^{4+} are 0.62 and 0.605 Å, respectively. In addition, they also found a finer domain structure in Ru-doped 0.9PZN–0.1PT, which may amplify the variation in refractive indices when the structure turns from the pure tetragonal phase into the hybrid tetragonal and cubic phase. Comparing the refractive indices of pure 0.9PZN–0.1PT with that of Ru-doped 0.9PZN–0.1PT, we can conclude that Ru-doped 0.9PZN–0.1PT is a more favorable medium for use in optical memories.

4. Conclusions

In this study, we observed the phase transitions of pure and Ru-doped 0.9PZN–0.1PT under heating through the measurement of their refractive indices by PME. From the experiments, we can conclude that when Ru is used as a dopant in 0.9PZN–0.1PT, the Curie region is broadened and shifts closer to room temperature. It is worthwhile to know that the use of an insulated chamber can completely eliminate heating problems for PEM, which has been a major drawback for PEM ellipsometry.

Acknowledgement

The authors acknowledge the funding from the National Science Council of Taiwan under grant number NSC 98-2221-E-009-024.

References

[1] M.E. Lines, A.M. Glass, Principles and Applications of Ferroelectric and Related Materials, Clarendon Press, Oxford, 1977.
[2] W. Cao, L.E. Cross, Phys. Rev. B 47 (1993) 4825.
[3] R. Guo, L.E. Cross, S.-E. Park, B. Noheda, D.E. Cox, G. Shirane, Phys. Rev. Lett. 84 (2000) 5423.
[4] W. Liu, X. Ren, Phys. Rev. Lett. 103 (2009) 257602.
[5] J. Kuwata, K. Uchino, S. Nomura, Jpn. J. Appl. Phys. 21 (1982) 1298.
[6] G. Shirane, S. Hoshino, K. Suzuki, Phys. Rev. 80 (1950) 1105.
[7] G. Xu, Z. Zhong, Y. Bing, Z.-G. Ye, G. Shirane, Nat. Mater. 5 (2006) 134.
[8] S.E. Park, T.R. Shrout, J. Appl. Phys. 82 (1997) 1804.
[9] D.E. Cox, B. Noheda, G. Shirane, Y. Uesu, K. Fujishiro, Y. Yamada, Appl. Phys. Lett. 79 (2001) 400.
[10] D. La-Orauttapong, B. Noheda, Z.-G. Ye, P.M. Gehring, J. Toulouse, D.E. Cox, G. Shirane, Phys. Rev. B 65 (2002) 144101.
[11] N. Setter, L.E. Cross, J. Appl. Phys. 51 (1980) 4356.
[12] J. Kuwata, K. Uchino, S. Nomura, Ferroelectrics 22 (1979) 863.
[13] I.A. Santos, J.A. Eiras, J. Phys. Condens. Matter 13 (2001) 11733.
[14] K. Buse, H. Hesse, U. van Stevendaal, S. Loheide, D. Sabbert, E. Krätzig, Appl. Phys. A Mater. Sci. Process. 59 (1994) 563.
[15] P.G. Clem, D.A. Payne, W.L. Warren, J. Appl. Phys. 77 (1995) 5865.
[16] C.H. Lin, C.Y. Huang, J.Y. Chang, Appl. Surf. Sci. 208–209 (2003) 340.
[17] F. Ramaz, L. Rakitina, M. Gospodinov, B. Briat, Opt. Mater. (Amsterdam, Neth.) 27 (2005) 1547.
[18] R. Fujimura, E. Kubota, O. Matoba, T. Shimura, K. Kuroda, Opt. Commun. 213 (2002) 373.
[19] C.H. Lin, C.Y. Huang, J.Y. Chang, Appl. Surf. Sci. 208–209 (2003) 340.
[20] V. Marinova, I. Ahmad, E. Goovaerts, J. Appl. Phys. 107 (2010) 113106.
[21] S.N. Jasperson, S.E. Schnatterly, Rev. Sci. Instrum. 40 (1969) 761.
[22] O. Acher, E. Began, B. Drevillon, Rev. Sci. Instrum. 60 (1989) 65.
[23] R.W. Collins, in: H.G. Tompkins, E.A. Irene (Eds.), Multichannel Ellipsometry, Handbook of Ellipsometry, William Andrew, New York, 2005, pp. 492–493.
[24] M.Y. Efremov, S.S. Soofi, A.V. Kiyanova, C.J. Munoz, P. Burgardt, F. Cerrina, P.F. Nealey, Rev. Sci. Instrum. 79 (2008) 043903.
[25] C.I. Chuang, Y.N. Hsiao, S.H. Lin, Y.F. Chao, Opt. Commun. 283 (2010) 3279.
[26] M.W. Wang, Y.F. Chao, Jpn. J. Appl. Phys. 41 (2002) 3981.
[27] M.W. Wang, Y.F. Chao, K.C. Leou, F.H. Tsai, T.L. Lin, S.S. Chen, Y.W. Liu, Jpn. J. Appl. Phys. 43 (2004) 827.
[28] T. Scholz, B. Mihailova, G.A. Schneider, N. Pagels, J. Hech, T. Malcherek, R.P. Fernandes, V. Marinova, M. Gospodinov, U. Bismayer, J. Appl. Phys. 106 (2009) 074108.
[29] Y.F. Chao, M.W. Wang, Z.C. Ko, J. Phys. D Appl. Phys. 32 (1999) 2246.
[30] H. Fujiwara, Spectroscopic Ellipsometry: Principles and Applications, John Wiley & Sons Ltd, West Sussex, England, 2007, 59 pp.
[31] G.A. Samara, E.L. Venturini, V. Hugo Schmidt, Phys. Rev. B 63 (2001) 184104.
[32] G. Yang, Z. Yue, Z. Gui, L. Li, J. Appl. Phys. 104 (2008) 074115.
[33] Y. Wu, M.J. Forbess, S. Seraji, S.J. Limmer, T.P. Chou, C. Nguyen, G. Cao, J. Appl. Phys. 90 (2001) 5296.
[34] J. Kim, J.G. Sung, H.M. Yang, B.W. Lee, J. Magn. Magn. Mater. 290–291 (2005) 1009.
[35] L.M. Wang, J.H. Lai, J.I. Wu, Y.K. Kuo, C.L. Chang, J. Appl. Phys. 102 (2007) 023915.
[36] F.S. Galasso, F.C. Douglas, R.J. Kasper, J. Chem. Phys. 44 (1966) 1672.
[37] C. Ritter, M.R. Ibarra, L. Morellon, J. Blasco, J. Garcia, J.M. De Teresa, J. Phys. Condens. Matter 12 (2000) 8295.